3D-Printed Viscoelastic Force-Limiting Connection for Seismic Protection of Nonstructural Components

Aaron Kang, Kaixin Chen, Georgios Tsampras
Department of Structural Engineering, University of California San Diego

BACKGROUND

Friction devices (FD) are used for seismic response modification, offering high initial stiffness, decoupled stiffness and strength, good energy dissipation, and the potential to be damage-free after earthquakes. However, conventional FDs have near-zero **post-elastic stiffness**, which can lead to excessive deformations when used as **force-limiting connections** between structural systems.

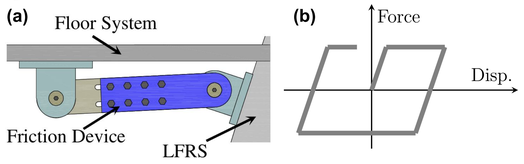


Figure 1. (a) Simplified side view of the FD[1-2] and (b) its expected force-displacement relationship

To address this, **low-damping rubber bearings** have been added externally to the connection system to provide post-elastic stiffness[1-2]. Yet, these bearings remain separate from the device itself.

This study integrates a post-elastic stiffening unit directly into a **3D-printed** friction device, creating a compact and lightweight solution that provides both energy dissipation and controlled post-elastic stiffness appropriate for **nonstructural components**.

SCOPE

- A new FD variant: **3DFD-Visco**, a 3D-printed, friction-based deformable connection made of **polyphthalamide carbon fiber** (PPA-CF) – a high-strength, lightweight 3D-printing filament suitable for nonstructural force demands
- Integrated viscoelastic component: A **thermoplastic polyurethane** (TPU) block is embedded directly into the assembly; TPU is **viscoelastic**, meaning its deformation depends on both load and time, providing rate-dependent energy dissipation.

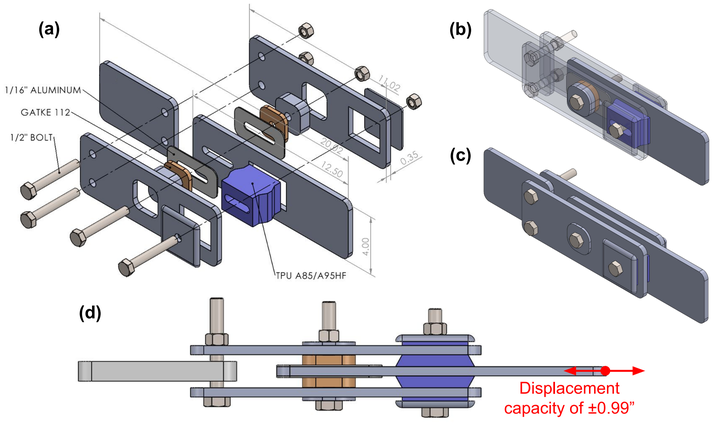


Figure 2. (a) Exploded view of 3DFD-Visco, (b) the assembly highlighting friction and TPU units, (c) the full assembly, and (d) the top view of the assembly

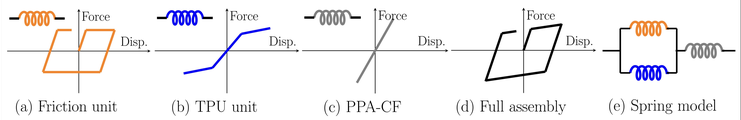


Figure 3. Force-displacement relationships for the 3DFD-Visco components and a simplified spring model of the full assembly

Objectives

- Evaluate experimentally and numerically the **hysteretic behavior** influenced by friction force as well as the Shore Hardness, infill, and geometry of the TPU
- Establish design guidelines for customizable, cost-effective, easily accessible, and scalable damping solutions for **nonstructural seismic applications**

METHODOLOGY

Table 1. List of materials in 3DFD-Visco

Component	Material	Qty.	Method of Fabrication
Internal plate	Bambulab PPA-CF	1	Bambu H2D
External plate	Bambulab PPA-CF	2	Bambu H2D
Friction shim plate	Bambulab PPA-CF	2	Bambu H2D
External bearing plate	Bambulab PPA-CF	2	Bambu H2D
TPU	Bambulab TPU A85 / TPU A95HF	1	Bambu X1-Carbon
External friction shim	Cotton-fiber composite (Gatke 112)	2	Onefinity CNC milling system
Internal sliding plate	Aluminum	2	Fablight FL4500 CNC laser cutter

The PPA-CF and TPU filaments were **blast dried** and printed under standard print parameters but only the PPA-CF was **annealed**.
JB Weld plastic adhesive was used based on its satisfactory **lap shear strength** capacity to fix the internal sliding plate to the internal plate. A load cell was bolted to each the friction and TPU unit to control the preload (how tight the unit was clamped).

Table 2. Pilot test matrix

Friction Bolt Preload	No TPU	40% Infill A85 TPU
0 kN	Completed	Completed
10 kN	Completed	Completed
20 kN	—	Failed

The assembly was subjected to five ±10 mm ramped sine wave loading protocols. The tests without TPU aimed to illustrate the behavior of solely the friction unit. The TPU bolt preload was 1 kN.

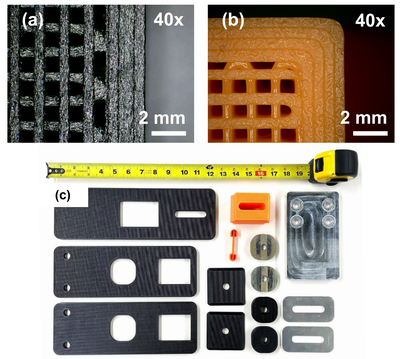


Figure 4. (a) Dino-Lite microscope image of 40% infill PPA-CF, (b) microscope image of 40% infill A85 TPU, and (c) 3DFD-Visco components

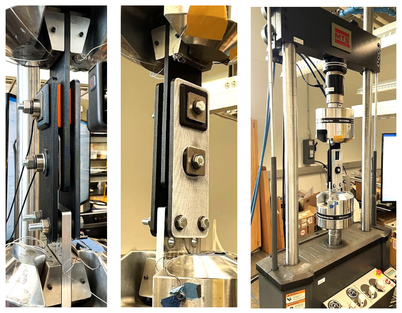
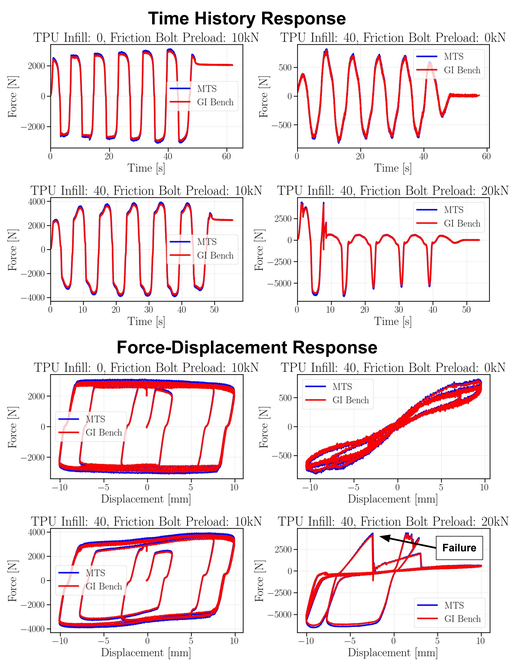


Figure 5. 3DFD-Visco on test rig

RESULTS



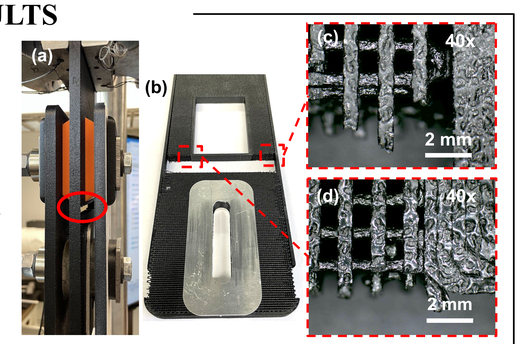


Figure 6. (a) and (b) Failure location on internal plate, (c) and (d) Dino-Lite microscope image of failure plane

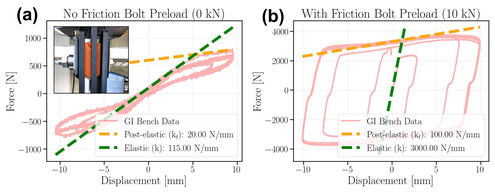
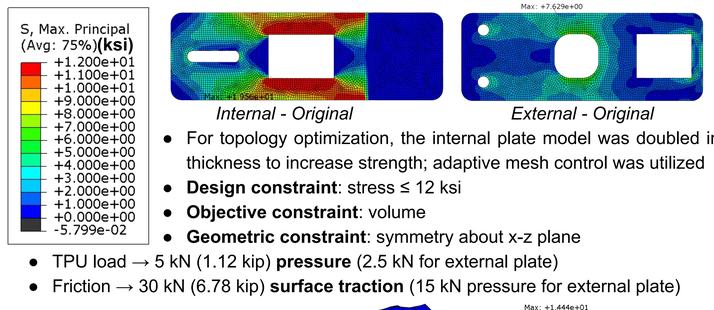


Figure 7. The force-displacement curves above highlight the stiffness, k, and the post-elastic stiffness, k_t, of (a) the TPU only and (b) the entire 3DFD-Visco assembly. The smaller k_t is attributed to the buckling of the extrusion on the TPU due to lateral compression.

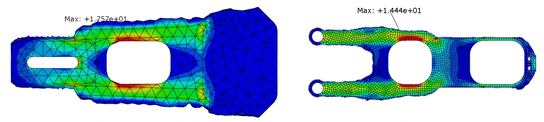
NUMERICAL STUDY

Static analysis of tested plates to determine the internal plate failure stress: σ =19.6 ksi



- For topology optimization, the internal plate model was doubled in thickness to increase strength; adaptive mesh control was utilized
- **Design constraint**: stress ≤ 12 ksi
- **Objective constraint**: volume
- **Geometric constraint**: symmetry about x-z plane
- TPU load → 5 kN (1.12 kip) **pressure** (2.5 kN for external plate)
- Friction → 30 kN (6.78 kip) **surface traction** (15 kN pressure for external plate)

Note: all contour plots show the tension load case (governing)



Assuming linear elastic theory, $F_{FEA} \propto \sigma_{FEA}$, where F_{FEA} is the applied force in Abaqus and σ_{FEA} is the corresponding maximum stress. The material failure stress $\sigma_{failure}$=19.6 ksi (from static analysis) can be used to calculate predicted failure force using Equation 1.

$$F_{\text{failure}} = n_{\text{plates}} F_{\text{FEA}} \times \frac{\sigma_{\text{failure}}}{\sigma_{\text{FEA}}} \quad (1)$$

Optimized internal plate with σ_{FEA}=17.6 ksi at F_{FEA}=30 kN: predicted $F_{failure}$ =33.4 kN.
Optimized external plate with σ_{FEA}=14.4 ksi at F_{FEA}=15 kN: predicted $F_{failure}$ =40.8 kN.

CONCLUSIONS AND FUTURE WORK

From the pilot test, as predicted, the friction unit induced energy dissipation while the TPU unit induced the post-elastic stiffening effect in the assembly.

- Sustained ±3.8 kN force under $F_{preload}$=10 kN
- Failed at +2.9 kN under $F_{preload}$=20 kN via block shear of internal plate at TPU region
- k_t/k ratio =0.174 (17.4%) for 40% infill A85 TPU, k_t/k =0.033 (3.3%) for full assembly
- Gatke 112 and aluminum friction coefficient ≈0.6 from filtering the data through a velocity threshold (dx/dt > 7 *mm/s*) and applying Equation 2.

$$\mu = \frac{F_{friction}}{n_{sliding}\, F_{preload}} \quad (2)$$

TPU blocks with modified geometry will be utilized in future tests to minimize corner stress concentrations

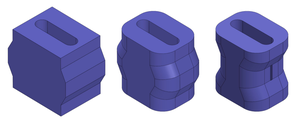


Figure 8. Original convex (left), filleted convex (middle), filleted concave (right) TPU shapes

3-D Digital Image Correlation (3D-DIC) analysis at the friction shim bearing location of the external plate was unsuccessful due to the insufficient speckle pattern on the infill surface. In the future it will be attempted to instead analyze the buckling area of the TPU.

ACKNOWLEDGEMENT

Special thanks to the Tsampras Research Group for their guidance and assistance with fabrication and testing, the UCSD Design and Innovation Building (DIB) Makerspace for providing access to the Fablight CNC laser, and Dr. Shivaglal Cheruvalath and Dr. Mary Thundathil of ScanPac Mfg., Inc. for generously donating the composite friction materials.

REFERENCES

[1] Tsampras G, Sause R, Fleischman RB, Restrepo JI. Experimental study of deformable connection consisting of friction device and rubber bearings to connect floor system to lateral force resisting system. Earthquake Engng Struct Dyn. 2018;47:1032–1053. https://doi.org/10.1002/eqe.3004
[2] Mayorga CF, Tsampras G. Reinforced concrete wall buildings with force-limiting connections: Modeling effects and uncertainty propagation. Earthquake Engng Struct Dyn. 2024;53:1465–1491. https://doi.org/10.1002/eqe.4073